

Stochastic model of the resistive switching mechanism in bipolar resistive random access memory: Monte Carlo simulations

A. Makarov^{a)}

Institute for Microelectronics, TU Wien, Gußhausstraße 27-29, 1040 Wien, Austria and Volgograd State Technical University, Lenin Avenue 28, 400131 Volgograd, Russia

V. Sverdlov^{b)} and S. Selberherr^{c)}

Institute for Microelectronics, TU Wien, Gußhausstraße 27-29, 1040 Wien, Austria

(Received 9 August 2010; accepted 25 October 2010; published 18 January 2011)

A stochastic model of the resistive switching mechanism in bipolar metal-oxide-based resistive random access memory (RRAM) is presented. The distribution of electron occupation probabilities obtained is in good agreement with previous work. In particular, it is shown that a low occupation region is formed near the cathode. Our simulations of the temperature dependence of the electron occupation probabilities near the anode and the cathode demonstrate a high robustness of the low and high occupation regions. This result indicates that a decrease in the switching time with increasing temperature cannot be explained only by reduced occupations of the vacancies in the low occupation region, but is rather related to an increase in the mobility of the oxide ions. A hysteresis cycle of a RRAM simulated with the stochastic model is in agreement with experimental results. © 2011 American Vacuum Society. [DOI: 10.1116/1.3521503]

I. INTRODUCTION

Memory based on charge storage (such as flash memory and others) is gradually approaching the physical limits of scalability. The increasing demand for minimization of microelectronic devices (e.g., MP3 players and mobile phones) has significantly accelerated the exploration of new concepts for nonvolatile memory during the past few years. Apart from good scalability a new type of memory must also exhibit low operating voltages, low power consumption, high operation speed, long retention time, high endurance, and simple structure.^{1,2}

Several concepts as potential replacements of the charge memory were proposed and developed. Some of the technologies are already available as prototype [such as carbon nanotube random access memory (RAM) and copper bridge RAM (CBRAM)], others as product [phase change RAM (PCRAM), magnetoresistive RAM, and ferroelectric RAM], while the technologies based on spin-torque transfer RAM, racetrack memory, and resistive RAM (RRAM) are under intensive research.

From these news concepts the CBRAM, PCRAM, and RRAM possess the simplest metal-insulator-metal structure. The electrical conductance of the insulator can be set at different levels by the application of an electric field. In CBRAM, PCRAM, and RRAM different types of materials are used. CBRAM is based on solid state electrolyte in which mobile metal ions may create a conductive bridge between the two electrodes under the influence of an electric field. PCRAM employs the difference in resistivity between crystalline and amorphous phases of a chalcogenide compound. RRAM is based on metal oxides, such as TiO_x ,³⁻⁶ HfO_2 ,⁷

Cu_xO ,⁸ NiO ,⁹ ZnO ,¹⁰ and perovskite oxides, such as doped SrTiO_3 ,¹¹ doped SrZrO_3 ,¹² and $\text{Pr}_{1-x}\text{Ca}_x\text{MnO}_3$.¹³

In addition to its simple structure RRAM is characterized by low operating voltage (<2 V), fast switching time (<10 ns), high density, and long retention time.

Several physical mechanisms based on either electron or ion switching have been recently suggested in literature: a model based on trapping of charge carriers,¹⁴ electrochemical migration of oxygen vacancies,^{15,16} electrochemical migration of oxygen ions,^{17,18} a unified physical model,¹⁹ a domain model,²⁰ a filament anodization model,²¹ a thermal dissolution model,²² a two-variable resistor model,²³ and others. Despite this, a proper fundamental understanding of the RRAM switching mechanism is still missing hindering further development of this type of memory.

In this work we present a stochastic model of the resistive switching mechanism based on electron hopping between the oxygen vacancies along the conductive filament in an oxide layer.

II. MODEL DESCRIPTION

We associate the resistive switching behavior in the oxide-based memory with the formation and rupture of a conductive filament (CF). The CF is formed by localized oxygen vacancies (V_O) (Ref. 19) or domains of V_O . Formation and rupture of a CF is due to a redox reaction in the oxide layer under a voltage bias. The conduction is due to electron hopping between these V_O (Fig. 1).

Figure 2 shows the unit cell of the two-dimensional (2D) model system. Columns with numbers 0 and $2N$ are reserved for the electrodes (there are generators and receivers of electrons in a model system). Places in odd-numbered columns at the intersections of the solid lines are reserved for oxygen vacancies V_O . An oxygen vacancy is formed, when an oxy-

^{a)}Electronic mail: makarov@iue.tuwien.ac.at

^{b)}Electronic mail: sverdlov@iue.tuwien.ac.at

^{c)}Electronic mail: selberherr@iue.tuwien.ac.at

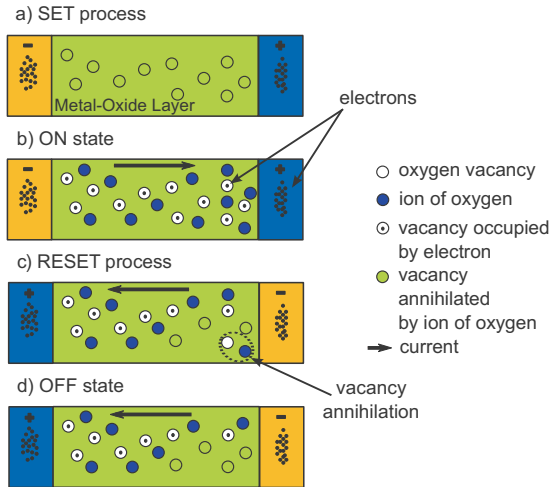


FIG. 1. (Color online) Illustration of the resistive switching mechanism in bipolar oxide-based memory cell: (a) schematic illustration of the set process, (b) schematic view of the conducting filament in the low resistance state (on state), (c) schematic illustration of the reset process, and (d) schematic view of the conducting filament in the high resistance state (off state). Only the oxygen vacancies and ions, which impact the resistive switching, are shown.

gen ion O^{2-} moves to a nearest empty interstitial position located at the intersections of the dotted lines (Fig. 2). An oxygen vacancy can be occupied by an electron hopping from another oxygen vacancy or from an electrode. Alternatively, an oxygen vacancy can be annihilated by an oxygen ion O^{2-} coming from a nearest interstitial position provided the vacancy is not occupied by an electron.

For modeling electrical conductivity in the low resistance state (i.e., when CF is formed) by a Monte Carlo technique,^{24,25} the following events are allowed:

- (1) an electron hop into V_O from an electrode,
- (2) an electron hop from V_O to an electrode, and
- (3) an electron hop between two V_O .

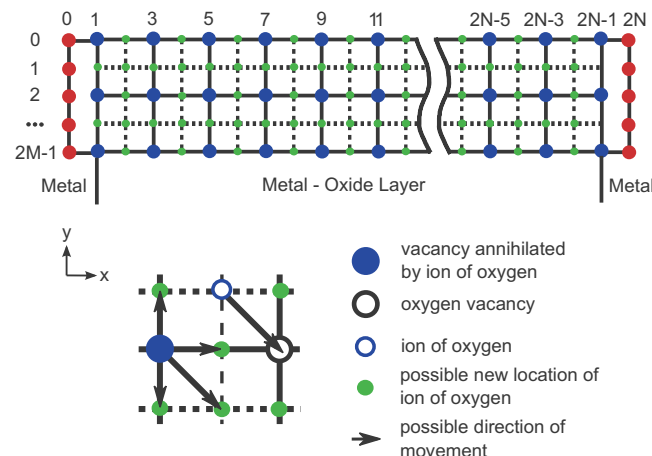


FIG. 2. (Color online) Schematic picture of the unit cell of the model system.

In order to model the dependences of transport on the applied voltage and temperature we choose the hopping rates for electrons as²⁶

$$\Gamma_{nm} = A_e \frac{\Delta E}{\hbar(1 - \exp(-\Delta E/k_B T))} \exp(-R_{nm}/a). \quad (1)$$

Here, \hbar is the Planck constant, A_e is a dimensionless coefficient, ΔE is the difference between the energies of an electron positioned at sites n and m , R_{nm} is the hopping distance, a is the localization radius, T is the temperature, and k_B is the Boltzmann constant. When an external voltage U is applied, the energy difference ΔE includes the corresponding voltage dependent term.

$$\Delta E = \frac{U}{d} \Delta x. \quad (2)$$

Here, d is the x -dimension of system, and $\Delta x = x_m - x_n$ is the difference between the x coordinate of the sites (vacancies) m and n .

Rates (1) are similar to those used in a single-electron transport theory.²⁵ An exponential in the denominator guarantees an exponentially small equilibrium occupation of a site m as compared to the occupation of a site n , if the condition $E_m - E_n \gg k_B T$ is satisfied. When the opposite condition $E_n - E_m \gg k_B T$ is fulfilled, the rate is proportional to the external field U/d . Therefore, rates (1) can mimic an Ohmic (linear in external field) transport in a system of equivalent sites having the same energy, if the temperature T considered as a parameter is set to zero.

To further specify the electron dynamics, we assume an electron hop from the site n to the site m may occur only, if the site n was occupied and the site m was empty before the hopping event. This is a manifestation of the fact that the energy gap separating the vacancies with one and two electrons is assumed large enough that the double occupancy of a vacancy becomes prohibitively small.

The hopping rates between an electrode (0 or $2N$) and an oxygen vacancy m are described by¹⁹

$$\Gamma_{0m}^{iC} = \alpha \Gamma_{0m}, \quad \Gamma_{m0}^{oC} = \alpha \Gamma_{m0}, \quad (3)$$

$$\Gamma_{(2N)m}^{iA} = \beta \Gamma_{(2N)m}, \quad \Gamma_{m(2N)}^{oA} = \beta \Gamma_{m(2N)}. \quad (4)$$

Here, α and β are the coefficients of the boundary conditions on the cathode and anode, respectively, N is the number of sites, A and C stand for cathode and anode, respectively, and i and o for hopping on the site and out from the site. Contrary to an oxygen vacancy, an electrode is assumed to have enough electrons so that hopping from an electrode to a vacancy is always allowed, provided the vacancy was empty before the event. Complimentary, an electrode has always a place to accept a carrier, so an electron can always hop at an electrode provided this event is allowed.

The current generated by hopping is calculated as

$$I = q_e \frac{\sum \Delta x}{d \sum t}. \quad (5)$$

Here, q_e is the electron charge, $t = (\sum_{m,n=0}^{2N} \Gamma_{nm} f_m (1-f_n))^{-1}$ is the time spent for moving an electron at a distance Δx , $f_n = 1(0)$, if the site n is occupied (empty), $f_0 = \alpha$ and $f_{2N} = \beta$, if an electron hops from an electrode, and $(1-f_0) = \alpha$ and $(1-f_{2N}) = \beta$, if a hop to an electrode occurs. Thus, $q_e \Delta x / d$ is a charge passing through an external circuit during a single hopping event.²⁴ The summation in Eq. (5) is over the whole hopping events. Therefore, Eq. (5) gives the current as the total charge passing through the external circuit during the total time $\sum t$ divided by the total time.

III. MODEL VERIFICATION

All calculations are carried out on one or/and two-dimensional lattices, and the distances between two nearest neighboring V_O in all directions are equal. All V_O are at the same energy level, if no voltage or temperature is applied. Despite the fact that in the binary metal oxides oxygen vacancies can have three different charge states with charges 0, +1, and +2, to simplify the model, we assume that the oxygen vacancy is either empty or occupied by one electron.¹⁹ This assumption is not a limitation, however, since, due to an energy separation between the three charge states, only two of them will be relevant for hopping and significantly contribute to transport.

A. Calculation of electron occupation probability

In order to verify the proposed model, we first evaluate the average electron occupations of hopping sites under different conditions. For comparison with previous works all calculations in this subsection are made on a one-dimensional lattice consisting of 30 equivalent, equidistantly positioned hopping sites V_O . For all simulations the localization radius is taken to be equal to 2 in units of the lattice constant.

At the initial moment of time we assume all sites to be empty. Electrons can hop from the cathode or anode positioned at 0 and $2N$, respectively, provided the rate of this transition is nonzero. After the time interval t each site in the lattice will be either occupied by an electron or empty. In the following instance each electron will have a probability Γ_{nm} of hopping from the site n to the site m , provided the target site m is empty; moreover, an electron may enter the lattice at site m from the cathode with the probability $\alpha \Gamma_{0m}$ or from the anode with the probability $\beta \Gamma_{(2N)m}$ (if this site m is empty) and an electron at site n may leave the lattice and hop to the cathode or the anode with the probability $\alpha \Gamma_{n0}$ or $\beta \Gamma_{n(2N)}$, respectively.

We have calibrated the model in a manner to reproduce the results reported in Ref. 19 for $V=0.4-1.6$ V. Figure 3(a) shows a case, where the hopping rate between the electrodes and V_O is larger than the rate between the two V_O (i.e., $\alpha, \beta > 1$). In this case the low occupation region is formed near the anode (unipolar behavior).

Figure 3(b) shows a case, where the hopping rate between the two V_O is larger than the rate between the electrodes and V_O (i.e., $\alpha, \beta < 1$). In this case a low occupation region is

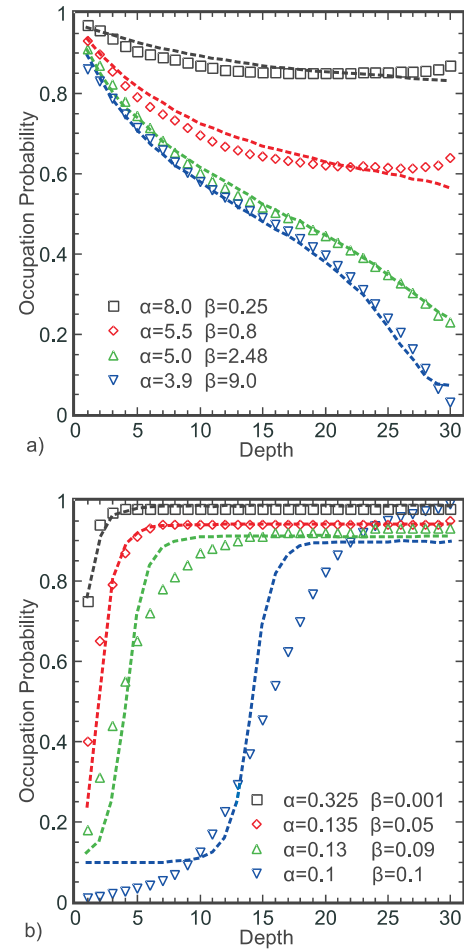


FIG. 3. (Color online) Calculated distribution of electron occupation probabilities under different biasing voltages. The lines are from Ref. 19. The symbols are obtained from our stochastic model.

formed near the cathode (bipolar behavior). The last curve for $\alpha=0.1$ and $\beta=0.1$ could be reproduced only with a localization radius equal to 6.

The values of the coefficients of the boundary conditions are determined by the materials from which the electrode and the oxide layer are made. A dependence of resistive switching on the electrode material was recently reported for ZrO_2 (Ref. 27) and TiO_2 .²⁸

Note that when $V=0$ V, the probability of occupation of all vacancies becomes equal to 0.5 regardless of the conditions applied before. According to Ref. 19 high electron occupation of an oxygen vacancy prevents the occupied vacancy from being annihilated by means of O^{2-} moving at V_O , thus preserving CF from rupture. The fact that an electron occupation probability of any vacancy decreases rapidly from 1 to 0.5 indicates that the probability of a CF rupture would increase substantially after the voltage is turned off. In the experiment, however, this is not observed. It indicates that a concept of CF stability/rupture based only on the high/low electron occupation of oxygen vacancies is not sufficient to explain the CF retention, and a generalization of the model to include the motion of ions must be considered.

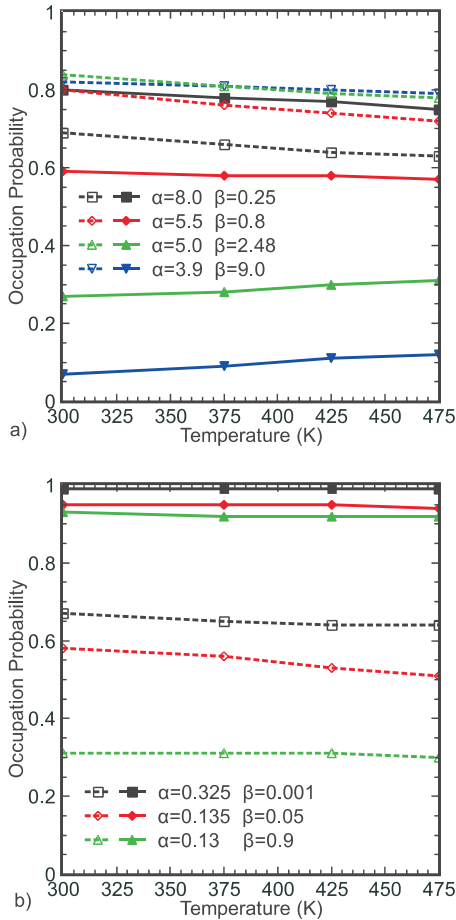


FIG. 4. (Color online) Temperature dependence of electron occupation probability near the anode (filled symbols) and the cathode (open symbols).

B. Modeling the temperature dependence

With the model calibrated in the manner to reproduce the results from Ref. 19 as described above we simulated the temperature dependence of the site occupations in the low occupation region. The results shown in Figs. 4(a) and 4(b) indicate high robustness of the low occupation region demonstrating changes in less than 10%, when the temperature is elevated from 25 to 200 °C. At the same time our finding indicates that the measured decrease in switching time with increasing temperature reported in Ref. 19 may stem from the increased mobility of oxide ions rather than from the occupations of V_O reduction in the low occupation region.

C. Modeling the reset process

Results obtained from simulations of the temperature dependence of the site occupations in the low occupation region demonstrate the necessity to include the dynamics of oxygen ions.

For modeling the resistive switching in oxide-based memory, in addition to the possible events of moving an electron, described above, we introduce the dynamics of oxygen ions (O^{2-}) as follows:

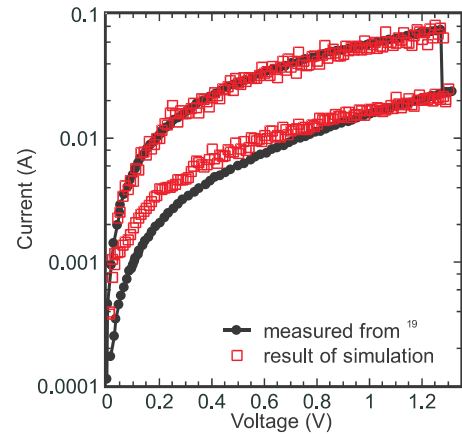


FIG. 5. (Color online) Current-voltage curves during the reset process. The lines are measured result from Ref. 19. The symbols are obtained from our stochastic model.

- (1) formation of V_O by O^{2-} moving to an interstitial position, and
- (2) annihilation of V_O by moving O^{2-} to V_O .

To describe the field-induced ion dynamics we have chosen the ion rates similar to Eq. (1) as follows:

$$\Gamma'_n = A_i \frac{\Delta E}{\hbar(1 - \exp(-\Delta E/k_b T))}. \quad (6)$$

Here we assume that O^{2-} can move from the lattice site to the nearest interstitial provided the interstitial is empty. Alternatively, O^{2-} can move back from the interstitial to the nearest vacancy, provided it is not occupied by an electron. A distance-dependent term is thus included in the dimensionless coefficient A_i . When the external voltage is applied, the difference in energy of an ion after and before hopping is computed as

$$\Delta E = \frac{U}{d}x - E_c. \quad (7)$$

E_c is a threshold energy for the m th vacancy V_O /annihilation energy of the m th vacancy V_O , when O^{2-} is moving to an interstitial or back to V_O , respectively. The values of these energies depend on the insulating material.

In order to verify the model, we simulated the reset I - V characteristics for a single-CF device.¹⁹

For modeling a single-CF system we use a one-dimensional lattice consisting of 30 equivalent, equidistantly positioned hopping sites V_O . To provide a possibility of vacancies to annihilate, we placed an oxygen ion near each V_O . For simulations the ratio A_i/A_e is equal to 10^{-3} .

In the first moment of time all V_O are formed and assumed to be unoccupied by electrons. Electrons can enter/leave the system and hop from/to an electrode, respectively, or hop between two V_O according to the rules described above (1–4). Each O^{2-} has a probability Γ'_n of annihilation with the nearest V_O if this V_O is not occupied by an electron. Figure 5 shows the simulation results of the reset process, which are in good agreement with the measurements from Ref. 19.

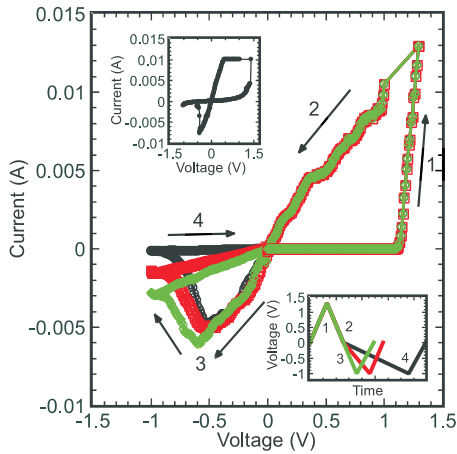


FIG. 6. (Color online) I - V characteristics showing the hysteresis cycle obtained from the stochastic model for different reset times ($\alpha=0.1$ and $\beta=0.1$). The inset (top) shows the hysteresis cycle for M - ZnO - M from Ref. 10. The inset (bottom) shows a schematic illustration of voltage V applied.

IV. RESULTS: MODELING OF THE HYSTERESIS CYCLE

In real systems formation of several CFs is possible. To allow this formation we now use a two-dimensional system with $N=30$ and $M=10$ shown in Fig. 2. We have investigated the I - V hysteresis by applying a sawtoothlike voltage V . The coefficients of the boundary conditions are constant and taken to be equal to 0.1.

The RRAM switching hysteresis cycle is shown in Fig. 6. The simulated cycle is in agreement with the experimental cycle from Ref. 10 shown in the inset (top) of Fig. 6. The interpretation of the RRAM hysteresis cycle obtained from the stochastic model is as follows. If a positive voltage is applied, the formation of a CF begins, when the voltage reaches a critical value sufficient to create V_O by moving O^{2-} to an interstitial position. The formation of the CF leads to a sharp increase in the current (Fig. 6, segment 1) signifying a transition to a state with low resistance. When a reverse negative voltage is then applied, the current increases linearly, until the applied voltage reaches the value at which an annihilation of V_O is triggered by means of moving O^{2-} to V_O . The CF is ruptured and the current decreases (Fig. 6, segment 3). This is the transition to a state with high resistance.

The increase in dimension of the system makes it possible to move from a model system to a more realistic structure. In order to highlight the dependence of the reset process on time the voltage is applied, we use the same voltage amplitude V but different time intervals. A schematic illustration of voltages V applied is shown in the inset (bottom) of Fig. 6. The results displayed in Fig. 6 clearly indicate that the proper CF rupture during the reset process is achieved, when the product “voltage-time” is maximal.

V. CONCLUSION

In this work we have presented a stochastic model of the bipolar resistive switching mechanism. The distribution of

the electron occupation probabilities calculated with the model is in good agreement with previous work. The simulated RRAM switching hysteresis cycle is in agreement with the experimental result. We have shown that the process of rupture of the CF is determined by the dynamics of oxygen ions and not only by the formation of the low occupation region. The proposed stochastic model can be used for performance optimization of RRAM devices.

ACKNOWLEDGMENT

The work is supported by the European Research Council through Grant No. 247056 MOSILSPIN.

- ¹B. C. Lee, P. Zhou, J. Yang, Y. T. Zhang, B. Zhao, E. Ipek, O. Mutlu, and D. Burger, *IEEE MICRO* **30**, 143 (2010).
- ²M. H. Kryder and C. S. Kim, *IEEE Trans. Magn.* **45**, 3406 (2009).
- ³C. Kugeler, C. Nauenheim, M. Meier, A. Rudiger, and R. Waser, *Non-Volatile Memory Technology Symposium, NVMTS*, 2008, 9th Annual, p. 6.
- ⁴L. E. Yu, S. Kim, M. K. Ryu, S. Y. Choi, and Y. K. Choi, *IEEE Electron Device Lett.* **29**, 331 (2008).
- ⁵D. S. Jeong, H. Schroeder, U. Breuer, and R. Waser, *J. Appl. Phys.* **104**, 123716 (2008).
- ⁶H. Shima, N. Zhong, and H. Akinaga, *Appl. Phys. Lett.* **94**, 082905 (2009).
- ⁷Y. S. Chen, T. Y. Wu, and P. J. Tzeng, 2009 International Symposium on VLSI Technology, Systems and Applications (VLSI-TSA), 2009, pp. 37 and 38.
- ⁸R. Dong, D. S. Lee, W. F. Xiang, S. J. Oh, D. J. Seong, and S. H. Heo, *Appl. Phys. Lett.* **90**, 042107 (2007).
- ⁹S. Seo *et al.*, *Appl. Phys. Lett.* **86**, 093509 (2005).
- ¹⁰S. Lee, H. Kim, D. J. Yun, S. W. Rhee, and K. Yong, *Appl. Phys. Lett.* **95**, 262113 (2009).
- ¹¹Y. Watanabe, J. G. Bednorz, A. Bietsch, Ch. Gerber, D. Widmer, A. Beck, and S. J. Wind, *Appl. Phys. Lett.* **78**, 3738 (2001).
- ¹²C. C. Lin, C. Y. Lin, and M. H. Lin, *IEEE Trans. Electron Devices* **54**, 3146 (2007).
- ¹³A. Sawa, T. Fujii, M. Kawasaki, and Y. Tokura, *Appl. Phys. Lett.* **85**, 4073 (2004).
- ¹⁴T. Fujii, M. Kawasaki, A. Sawa, H. Akoh, Y. Kawazoe, and Y. Tokura, *Appl. Phys. Lett.* **86**, 012107 (2005).
- ¹⁵Y. B. Nian, J. Strozier, N. J. Wu, X. Chen, and A. Ignatiev, *Phys. Rev. Lett.* **98**, 146403 (2007).
- ¹⁶S. X. Wu, L. M. Xu, and X. J. Xing, *Appl. Phys. Lett.* **93**, 043502 (2008).
- ¹⁷K. Szot, W. Speier, G. Bihlmayer, and R. Waser, *Nature Mater.* **5**, 312 (2006).
- ¹⁸Y. Nishi and J. R. Jameson, *Device Research Conference*, 2008 (unpublished), pp. 271–274.
- ¹⁹B. Gao, B. Sun, H. Zhang, L. Liu, X. Liu, R. Han, J. Kang, and B. Yu, *IEEE Electron Device Lett.* **30**, 1326 (2009).
- ²⁰M. J. Rozenberg, I. H. Inoue, and M. J. Sanchez, *Phys. Rev. Lett.* **92**, 178302 (2004).
- ²¹K. Kinoshita, T. Tamura, H. Aso, H. Noshiro, C. Yoshida, M. Aoki, Y. Sugiyama, and H. Tanaka, *Non-Volatile Semiconductor Memory Workshop, IEEE NVSMW 2006*, 21st, pp. 84 and 85.
- ²²U. Russo, D. Ielmini, C. Cagli, A. L. Lacaita, S. Spiga, C. Wiemer, M. Perego, and M. Fanciulli, *Tech. Dig. - Int. Electron Devices Meet.* **2007**, 775.
- ²³S. Kim and Y. K. Choi, *IEEE Trans. Electron Devices* **56**, 3049 (2009).
- ²⁴A. N. Korotkov and K. K. Likharev, *Phys. Rev. B* **61**, 15975 (2000).
- ²⁵K. K. Likharev, N. S. Bakhvalov, G. S. Kazacha, and S. I. Serduykova, *IEEE Trans. Magn.* **25**, 1436 (1989).
- ²⁶V. Sverdlov, A. N. Korotkov, and K. K. Likharev, *Phys. Rev. B* **63**, 081302 (2001).
- ²⁷C. Y. Lin, C. Y. Wu, C.-Y. Wu, T. C. Lee, F. L. Yang, C. Hu, and T. Y. Tseng, *IEEE Electron Device Lett.* **28**, 366 (2007).
- ²⁸W. G. Kim and S. W. Rhee, *Microelectron. Eng.* **87**, 98 (2010).